Sensors and Materials, Vol. 37, No. 9 (2025) 3829–3839
MYU Tokyo

S & M 4155

Flood Susceptibility Mapping Using Machine Learning Models with Novel Flood Inventory Sampling Strategies

Gen Long,[1†] Sarintip Tantanee,[2*] Korakod Nusit,[1] and Pitikhate Sooraksa[3]

[1]Civil Engineering Department, Faculty of Engineering, Naresuan University, Phitsanulok 65000, Thailand
[2]Center of Excellence on Energy Technology and Environment, Faculty of Engineering, Naresuan University, Phitsanulok 65000, Thailand
[3]Department of Robotics and AI, School of Engineering, King Mongkut's Institute of Technology Ladkrabang, 1 Chalongkrung 1, Ladkrabang, Bangkok 10520, Thailand

(Received February 3, 2025; accepted May 26, 2025)

Keywords: flood susceptibility, machine learning, random forest, ensemble learning

In this study, we introduce an innovative frequency-area-weighted sampling method to address spatial and temporal biases in flood inventory creation. Focusing on Thailand's Nan River Basin, we integrated 13 flood conditioning factors and developed a point-based inventory that includes 3000 flood and 3000 non-flood samples, proportionally allocated on the basis of flood recurrence intervals and spatial distribution. We evaluated four machine learning models—artificial neural network, support vector machine, K-nearest neighbors, and random forest (RF) models—to assess their performance in flood susceptibility mapping (FSM). Among these, the RF model demonstrated the highest predictive capability, achieving an area under the curve (AUC) of 0.979 for the test set and an AUC of 0.984 for the verification set. The resulting susceptibility map identified 10.64% of the study area as "very high" risk, providing critical insights for prioritizing flood mitigation efforts. This work advances FSM methodology by effectively bridging the temporal flood frequency and spatial heterogeneity in inventory design, offering a robust framework for data-driven flood risk management in vulnerable regions.

1. Introduction

Floods rank among the most devastating natural disasters, causing catastrophic economic losses, infrastructure damage, and threats to human safety.(1,2) Predicting flood risks is thus critical to ensuring the resilience of communities in flood-prone areas. Flood susceptibility mapping (FSM) has become an essential tool for assessing and mitigating these risks, providing decision-makers with critical information to design effective flood management strategies and allocating resources efficiently.(3,4) FSM helps identify areas that are more likely to be affected by floods, which is crucial for disaster preparedness, urban planning, and environmental conservation.

The Nan River Basin in Northern Thailand faces significant flood risks, impacting both human settlements and agriculture. Studies such as those by Tingsanchali and Promping(5) and

*Corresponding author: e-mail: sarintipt@nu.ac.th
†Present address: School of Science and Technology, Pu'Er University, Yunnan Province, China, 665000
https://doi.org/10.18494/SAM5586

ISSN 0914-4935 © MYU K.K.
https://myukk.org/

Amnatsan *et al.*(6) highlight increasing flood risk with longer return periods, especially in urban areas like Nan City. Nusit *et al.*(7) emphasized the vulnerability of Phitsanulok City owing to its high population density and economic activities. However, most research has focused on smaller-scale areas without new techniques such as machine learning (ML) methods that focus on basin-wide scales. These gaps underscore the need for comprehensive flood risk evaluations to guide large-scale mitigation efforts.

Traditionally, FSM has relied on multi-criteria decision analysis (MCDA) and statistical methods to assess flood risk. While these approaches are widely used, they have limitations. MCDA often requires subjective weighting of criteria, which introduces bias, while statistical methods may not fully account for the complex spatial and temporal patterns of flooding.(3) In recent years, ML techniques have emerged as powerful alternatives that offer the ability to model flood susceptibility more accurately by recognizing patterns in large and complex datasets. Prominent ML algorithms used in FSM include artificial neural networks (ANNs),(8) support vector machines (SVMs),(9) K-nearest neighbors (KNNs),(10) and random forests (RFs).(11) Unlike conventional methods, ML algorithms can capture nonlinear relationships and handle high-dimensional data without requiring prior assumptions about underlying processes.(12)

However, the accuracy and reliability of ML-based FSM models are heavily dependent on the quality and representativeness of flood inventory data. Panyadee and Champrasert(13) stressed that flood hazard maps are often accurate only for specific periods and may become outdated, emphasizing the unpredictable nature of disasters and the necessity for real-time data to ensure accurate and responsible disaster predictions. Incorporating multiyear flood data can mitigate these temporal biases, capturing variations and trends over time and thereby enhancing the robustness of FSM models.

The objective of this study is to develop a reliable flood susceptibility map for the Nan River Basin in Northern Thailand using ML techniques. A key innovation is the proposed frequency-area-weighted sampling method, wherein sampling weights are quantified through a joint metric of flood recurrence intervals and their spatial extents, which addresses the under-representation of heterogeneous flood patterns. We compare four ML models—ANN, SVM, KNN, and RF—to evaluate their performances for FSM in the study area.

2. Study Area

The Nan River Basin (Fig. 1) in northern Thailand spans approximately 34269 km^2 and features a mix of mountainous terrains and river floodplains. The Nan River, the basin's main watercourse, extends about 770 km and plays a crucial role in the region's hydrology. Because of its topography and seasonal rainfall patterns, the basin is prone to flood risks, particularly during the rainy season. Nan River's high flow variability, coupled with rapid urbanization and agricultural activities, increases the area's vulnerability to flood events.(14,15) Historical records indicate that the basin has faced recurring floods, notably in 2006 and 2011, resulting in substantial damage and casualties.(5) These events underscore the importance of effective flood risk management strategies for sustainable development and disaster prevention.

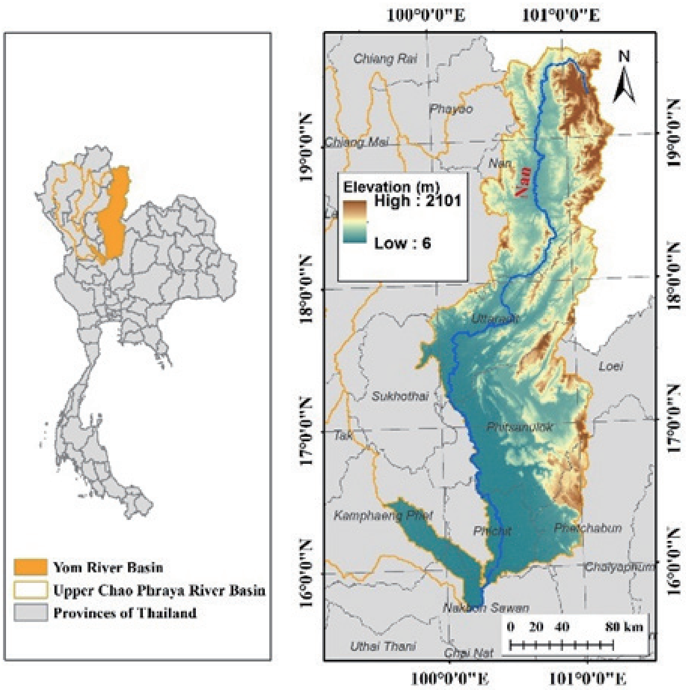

Fig. 1. (Color online) Study area.

3. Methodology

As shown in Fig. 2, the methodology used in the current study can be divided into data acquisition and preprocessing, data processing, ML modeling, and evaluation.

3.1 Data acquisition and preprocessing

This phase involves flood inventory and flood conditioning factor (FCF) data acquisition and preprocessing. The historical flood data was obtained from the Geo-Informatics and Space Technology Development Agency (GISTDA) of Thailand, which covers a period of 17 years from 2006 to 2022 in polygon format. To construct a point-based inventory dataset, as shown in Fig. 3, we allocate 3000 flood [Fig. 3(a)] and 3000 non-flood [Fig. 3(b)] samples proportionally on the basis of yearly flood recurrence and their spatial extents. The number of samples for each flood event (N_i) was determined using Eq. (1).

$$N_i = \frac{F_i \times A_i}{\sum (F_i \times A_i)} \times 3000, \tag{1}$$

where F_i denotes the recurrence interval and A_i represents the spatial extent of the ith flood event. This method ensures that events involving larger areas and more frequent occurrences are

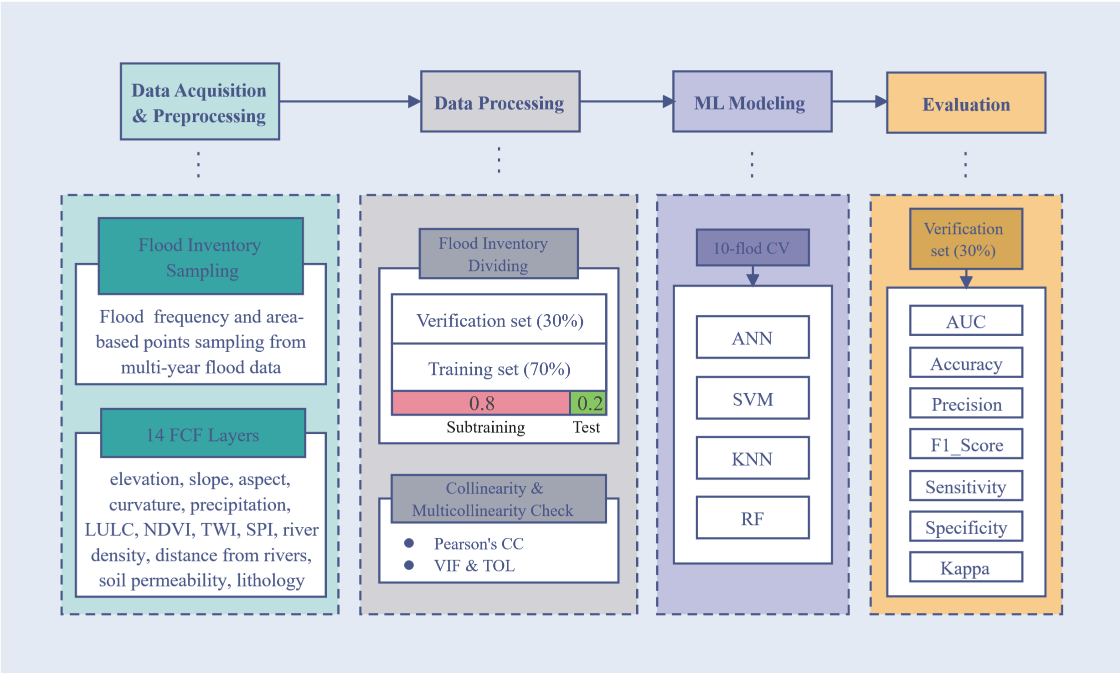

Fig. 2. (Color online) Methodology workflow.

F_i	A_i (km^2)	N_i
0	29047.42	3000
1	1628.44	215
2	1048.74	277
3	766.00	304
4	585.01	309
5	437.62	289
6	310.32	246
7	213.09	197
8	149.94	159
9	112.18	133
10	90.04	119
11	86.72	126
12	116.31	185
13	92.27	159
14	151.76	282

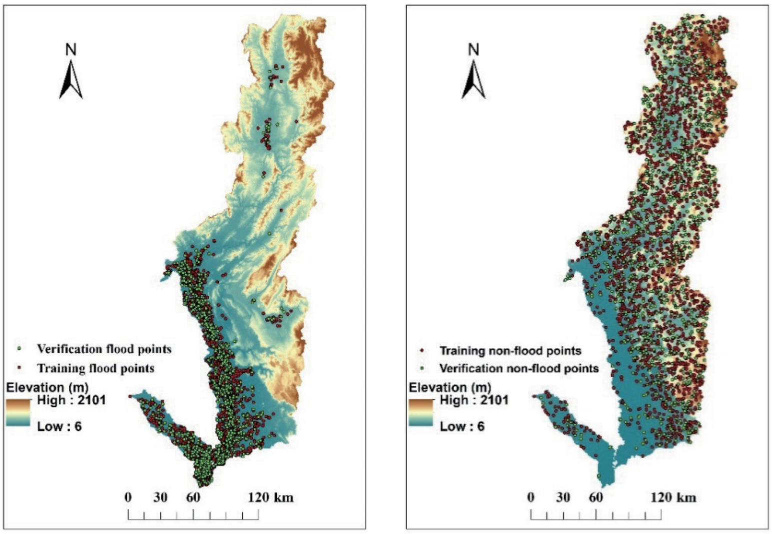

(a) (b)

Fig. 3. (Color online) Sampled 3000 flooded (a) and 3000 non-flood (b) point inventory.

adequately represented in the sample set. Non-flood samples were randomly selected from areas not affected by recorded flood events, ensuring a balanced representation of both flood-prone and non-flood-prone zones within the basin.

Selecting appropriate FCFs is crucial for enhancing flood prediction accuracy. In the literature, these factors are categorized into topographic, hydrological, climatic, and anthropogenic groups.[16] The relevance of specific FCFs varies depending on the watershed characteristics, making their careful selection vital for effective flood modeling.[11] In this study, we selected 13 commonly used FCFs: elevation, slope, aspect, curvature, precipitation, land use/land cover (LULC), normalized difference vegetation index (NDVI), topographic wetness index (TWI), stream power index (SPI), river density, distance from river, soil permeability, and lithology.

The topographic factors—elevation, slope, aspect, curvature, TWI, and SPI—were derived from the Shuttle Radar Topography Mission (SRTM) DEM with a 30-meter resolution, available from the U.S. Geological Survey (USGS) EarthExplorer. The NDVI was generated using Landsat 8 OLI/TIRS Level-2 data, also accessible via the USGS EarthExplorer. Soil permeability data from 2018 and LULC data from 2021 were obtained from Thailand's Land Development Department (LDD). Average annual precipitation data for 1981–2022 was sourced from the Thai Meteorological Department. Distance from rivers and river density were calculated using river network data from 2017, provided by the Water Analysis and Assessment Division of Thailand's Department of Water Resources (DWR). Lithology data was sourced from the Generalized Geology of Southeast Asia dataset provided by the USGS.

3.2 Data processing

The flood inventory data was divided into training and validation sets, with 70% of the data randomly selected for training and the remaining 30% reserved for validation. The training set was further split, allocating 80% for subtraining and 20% as a test set. The test set was used during model training to assess performance and prevent overfitting, while the validation set was used to evaluate the model's generalization capability. All FCF data were standardized into a 30-meter raster format. To ensure the reliability of the model, we assessed the FCFs for multicollinearity using Pearson's correlation coefficients and variance inflation factor (VIF) methods. No multicollinearity issues were detected among the FCFs in this study.

3.3 ML modeling

This phase involves ANN, SVM, KNN, and RF modeling with 10-fold cross-validation (10-fold CV). The 70% flood inventory training dataset was used to train the following models.

- ANNs are ML models, inspired by the human brain, consisting of an input layer, one or more hidden layers, and an output layer. They process data through interconnected neurons with weighted connections, which are adjusted during training to minimize errors. ANNs are highly effective for modeling complex, nonlinear relationships, making them suitable for applications in, for example, FSM. They outperform many traditional statistical methods by capturing intricate patterns in data. Despite challenges like sensitivity to training data and limitations in extrapolating predictions, ANNs remain powerful tools for classification and regression tasks owing to their adaptability and ability to handle large datasets.[17–19]
- SVMs are supervised learning algorithms widely applied in FSM for classification and regression tasks. They find the optimal hyperplane that maximizes the margin of separation

between two classes. Using kernel functions, an SVM transforms nonlinear data into a higher-dimensional feature space, allowing for linear separation of complex patterns. Support vectors, the critical data points near the hyperplane, play a key role in determining the position and orientation of the hyperplane in SVM models. SVMs' ability to handle nonlinear relationships and achieve accurate classification makes them a reliable tool for flood susceptibility analysis and other predictive modeling tasks.[19,20]

- KNNs are simple, nonparametric algorithms used for supervised classification and regression. They operate on the principle that similar items are located near each other in space. In KNNs, the training phase involves storing the data without making assumptions; thus, they are referred to as "lazy learners". When classifying a new instance, KNNs are found on the basis of the Euclidean distance and assigned a class label through majority voting. A KNN model's performance depends on the choice of k and the search range, which directly influences the prediction results. It is widely used for classification tasks because of its simplicity and effectiveness.[21,22]
- RFs are ensemble ML algorithms widely used for supervised learning tasks like FSM. They combine two key techniques: bagging, which generates multiple predictors through bootstrapping and averages their predictions, and random feature selection, where a subset of features is chosen for each decision tree. An RF model builds multiple trees and uses majority voting for final predictions. It is effective for handling large datasets, missing values, and complex relationships. It uses k-fold cross-validation to tune hyperparameters such as the number of estimators and tree depth.[18,19]

3.4 Evaluation

In this phase, widely adopted and comprehensive statistical metrics, including AUC, accuracy, precision, F1 score, sensitivity, specificity, and kappa, were selected to evaluate the validity and performance of the models with the 30% verification flood inventory dataset. The results for the four models were compared to assess their performance.

4. Results and Discussion

The performances of four ML models—ANN, SVM, KNN, and RF—were evaluated in terms of their predictive ability for FSM. The results, as shown in Fig. 4 and Table 1, highlight the strengths and weaknesses of each model on the basis of various performance metrics and their ability to classify susceptibility levels.

Figure 4 shows the ROC curves for the ANN, SVM, KNN, and RF models on both the test and verification datasets. The RF model performed the best with an AUC of 0.979, followed by SVM (0.970), KNN (0.955), and ANN (0.951). On the verification dataset, RF again outperformed the others with an AUC of 0.984, closely followed by SVM (0.977). ANN and KNN showed AUC values of 0.965 and 0.958, respectively. Overall, RF consistently demonstrated the highest performance across both datasets, with SVM showing good results as well.

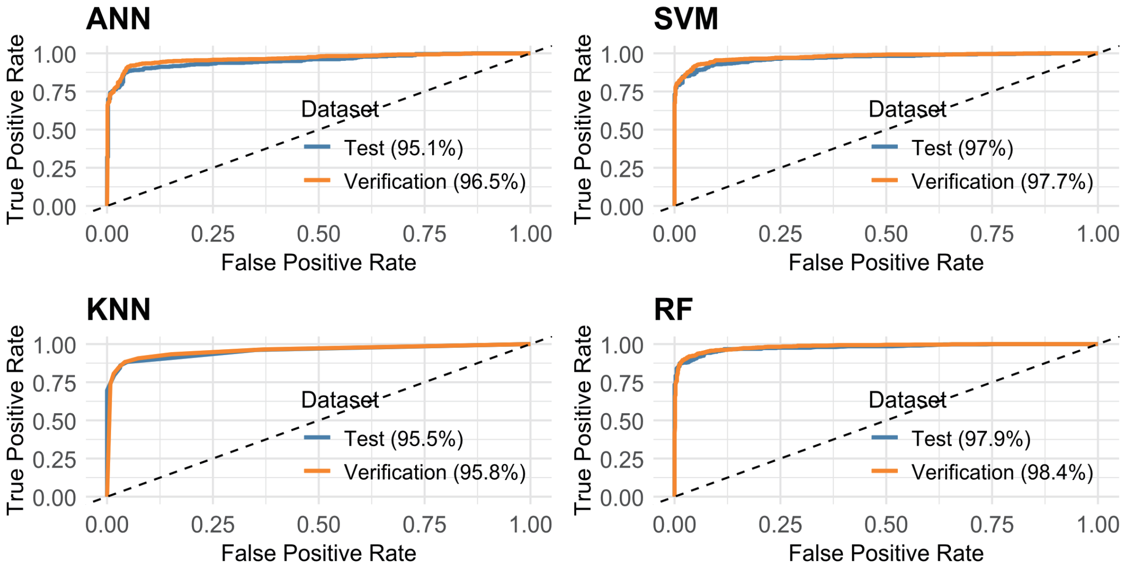

Fig. 4. (Color online) ROC curves of ANN, SVM, KNN, and RF models for test and verification datasets.

Table 1
Performance metrics of the ANN, SVM, KNN, and RF models.

Model	AUC	Accuracy	Precision	F1_Score	Sensitivity	Specificity	Kappa
Based on the test dataset (20% of the training set) with 10-fold cross-validation							
ANN	0.951	0.915	0.831	0.881	0.950	0.946	0.912
SVM	0.970	0.913	0.826	0.862	0.964	0.960	0.908
KNN	0.955	0.914	0.828	0.859	0.969	0.965	0.909
RF	0.979	0.926	0.852	0.893	0.960	0.957	0.923
Based on the verification dataset							
ANN	0.965	0.930	0.860	0.912	0.948	0.946	0.929
SVM	0.977	0.924	0.848	0.886	0.961	0.958	0.921
KNN	0.958	0.920	0.840	0.883	0.957	0.953	0.917
RF	0.984	0.939	0.878	0.923	0.954	0.953	0.938

Table 1 summarizes the performance metrics of the ANN, SVM, KNN, and RF models on both the test and verification datasets. For the test dataset, the RF model achieved the highest AUC (0.979), followed by SVM (0.970), KNN (0.955), and ANN (0.951). RF also demonstrated the highest accuracy (0.926), precision (0.852), F1 score (0.893), sensitivity (0.960), specificity (0.957), and kappa (0.923). In comparison, SVM, KNN, and ANN exhibited slightly lower but competitive performance across these metrics. For the verification dataset, RF continued to show superior performance, with an AUC of 0.984, accuracy of 0.939, precision of 0.878, and the highest F1 score (0.923). While SVM, KNN, and ANN showed strong performance with AUC values of 0.977, 0.958, and 0.965, respectively, RF consistently outperformed the other models across all metrics, demonstrating the best performance in flood susceptibility prediction.

Figure 5 shows the flood susceptibility maps generated by the ANN, SVM, KNN, and RF models, and Fig. 6 shows their respective areas (in km^2) and proportions of different susceptibility levels (very low, low, moderate, high, and very high). The ANN model [Fig. 5(a)]

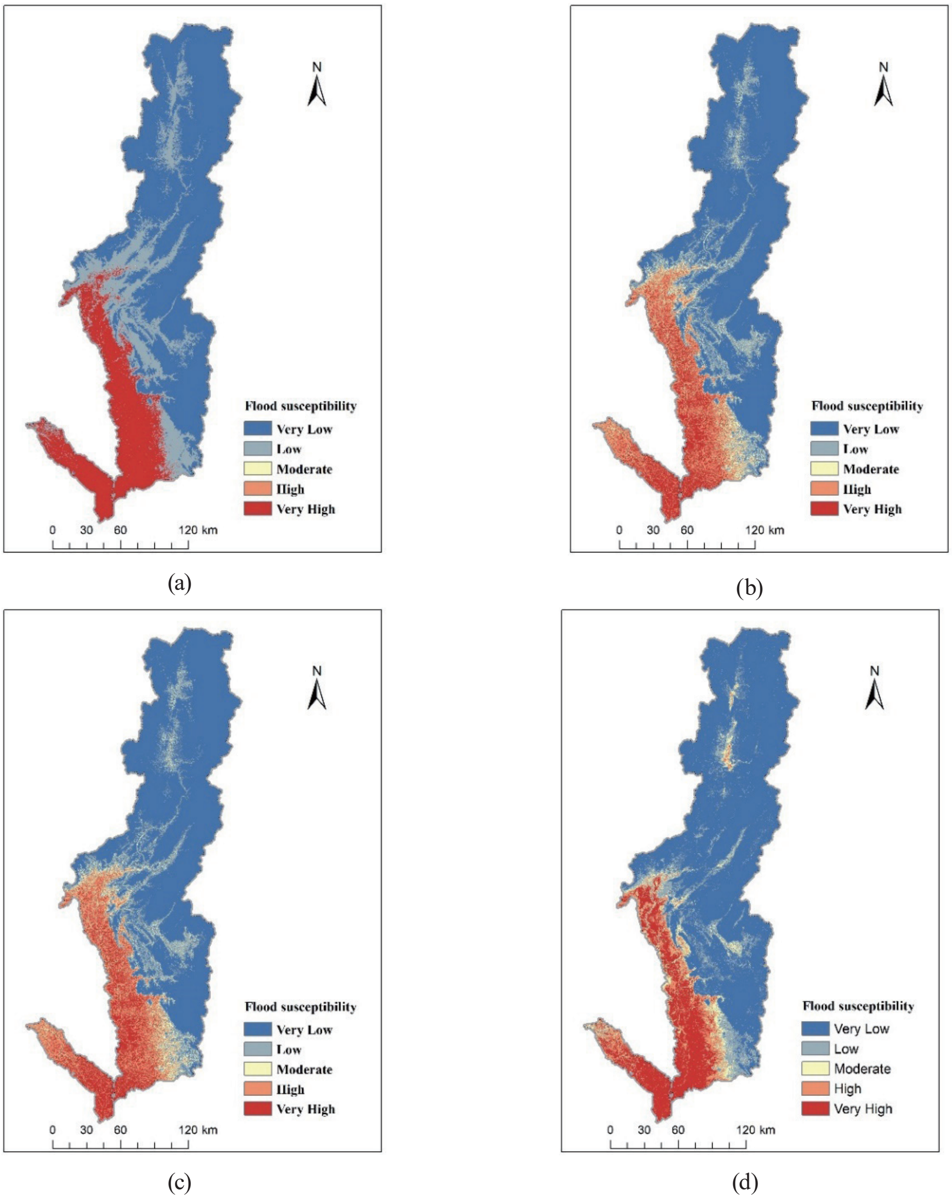

Fig. 5. (Color online) Flood susceptibility maps generated by (a) ANN, (b) SVM, (c) KNN, and (d) RF models.

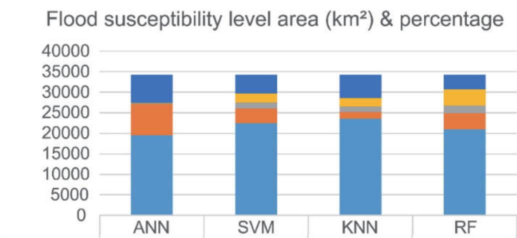

	ANN	SVM	KNN	RF
Very High	20.39%	13.37%	16.70%	10.64%
High	0.24%	6.44%	5.75%	11.41%
Moderate	0.25%	4.35%	3.88%	5.28%
Low	22.31%	10.20%	4.92%	11.47%
Very Low	56.81%	65.65%	68.75%	61.20%

Very Low Low Moderate High Very High

Fig. 6. (Color online) Areas and proportions of flood susceptibility levels mapped by the ANN, SVM, KNN, and RF models.

showed that the majority of the area was classified as having very low susceptibility (56.81%), with a small percentage as low (22.31%). Notably, the proportions of the area with moderate (0.25%) and high (0.24%) susceptibility levels were extremely small, highlighting that the model predominantly classified the area as having low susceptibility. The very high susceptibility area accounted for 20.39%.

In contrast, the SVM model [Fig. 5(b)] classified the largest portion of the area into having very low susceptibility (65.65%), with low-susceptibility areas covering 10.20% and a more balanced distribution across higher susceptibility levels, including 13.37% in the very high category. The KNN model [Fig. 5(c)] also showed a dominant proportion of the area with very low susceptibility (68.75%) but significant portions classified into the very high (16.70%) and low (4.92%) categories. The model showed slightly larger areas in the moderate (3.88%) and high (5.75%) susceptibility categories than the ANN model.

The RF model [Fig. 5(d)] had a more balanced distribution, with 61.20% of the area classified as very low, 11.47% as low, and significant areas in the moderate (5.28%) and high (11.41%) categories. The very high susceptibility level accounted for 10.64%, reflecting a more evenly spread susceptibility classification than in the other models. These results demonstrate how each model distributed susceptibility levels across the study area, with RF and SVM having more balanced distributions, while ANN and KNN focused more on very low susceptibility in very small areas in the higher susceptibility categories.

In summary, RF consistently outperformed the other models in terms of both overall accuracy and the ability to classify flood susceptibility. The model's ability to provide a well-balanced distribution of susceptibility classes and its superior performance across all evaluation metrics make it the most suitable choice for FSM in this study. This aligns with previous findings[9,12,23] that ensemble algorithms outperform stand-alone ML models. SVM also demonstrated high performance with high accuracy and AUC values, but its classification of susceptibility levels was more skewed towards very small areas compared with RF.

While ANN and KNN performed well, they showed some limitations, particularly in classifying higher-risk areas. ANN's tendency to classify areas as having very low susceptibility, with very small proportions classified into higher-susceptibility categories, may limit its applicability to accurate flood risk prediction. Similarly, KNN's high sensitivity but relatively low specificity suggests it may over-predict flood-prone areas in some instances.

These findings highlight the importance of selecting the right model for FSM, with RF emerging as the most robust and versatile model. The distribution of flood susceptibility levels observed in this study is crucial for planning flood management strategies, as it allows decision-makers to effectively identify both low-risk and high-risk areas.

5. Conclusions

We demonstrated the effectiveness of ML models in FSM and found RF to consistently outperform SVM, KNN, and ANN. RF achieved the highest AUC scores of 0.979 for the test dataset and 0.984 for the verification dataset, highlighting its robustness in predicting flood-prone areas within the study region.

Our research results also underscore the importance of integrating advanced ML algorithms with a diverse set of FCFs to enhance prediction accuracy. The observed distribution of flood susceptibility levels is crucial for planning effective flood management strategies, enabling decision-makers to identify both low-risk and high-risk areas efficiently.

Furthermore, the study revealed the significance of employing appropriate flood inventory sampling strategies in FSM. The proposed frequency-area-weighted sampling method, which allocates samples on the basis of flood recurrence intervals and their spatial extents, addresses the under-representation of heterogeneous flood patterns, thereby improving model accuracy. Future work should be focused on further improvement of the prediction accuracy by incorporating newer techniques such as stacking,(24) deep learning,(25) and other emerging AI methods.

Acknowledgments

This work was supported and funded by Naresuan University Faculty of Engineering Scholarships.

References

1 D. A. Week and C. H. Wizor: Asian J. Geogr. Res. **3** (2020) 1. https://doi.org/10.9734/ajgr/2020/v3i130096
2 U. Djanibekov, M. Polyakov, H. Craig, and R. Paulik: Econ. Disasters Clim. Change **8** (2024) 283. https://doi.org/10.1007/s41885-024-00147-3
3 C. M. Kaya and L. Derin: J. Water Clim. Change **14** (2023) 1935. https://doi.org/10.2166/wcc.2023.035
4 O. Rahmati, H. Darabi, M. Panahi, Z. Kalantari, S. A. Naghibi, C. S. S. Ferreira, A. Kornejady, Z. Karimidastenaei, F. Mohammadi, S. Stefanidis, D. Tien Bui, and A. T. Haghighi: Sci. Rep. **10** (2020) 12937. https://doi.org/10.1038/s41598-020-69703-7
5 T. Tingsanchali and T. Promping: Water **14** (2022) 161. https://doi.org/10.3390/w14020161
6 S. Amnatsan, J. S. M. Fowze, A. Bormudoi, M. K. Hazarika, and L. Samarakoon: 7th Annu. Mekong Flood Forum (2009) 297–303.
7 K. Nusit, S. Tantanee, K. Subsomboon, S. Leungvichcharoen, and S. Yiemwattana: Geogr. Technica **14** (2019) 129. https://dx.doi.org/10.21163/gt_2019.141.26
8 M. S. Rana and C. Mahanta: Nat. Hazards **115** (2022) 947. https://doi.org/10.1007/s11069-022-05580-9
9 B. Choubin, E. Moradi, M. Golshan, J. Adamowski, F. Sajedi-Hosseini, and A. Mosavi: Sci. Total Environ. **651** (2019) 2087. https://doi.org/10.1016/j.scitotenv.2018.10.064
10 J. Yao, X. Zhang, W. Luo, C. Liu, and L. Ren: Int. J. Appl. Earth Obs. Geoinf. **112** (2022) 102932. https://doi.org/10.1016/j.jag.2022.102932
11 K. Chapi, V. P. Singh, A. Shirzadi, H. Shahabi, D. T. Bui, B. T. Pham, and K. Khosravi: Environ. Modell. Software **95** (2017) 229. https://doi.org/10.1016/j.envsoft.2017.06.012
12 K. Gulshad, A. Yaseen, and M. Szydłowski: Remote Sens. **16** (2024) 3902. https://doi.org/10.3390/rs16203902
13 P. Panyadee and P. Champrasert: Sustainability **16** (2024) 4433. https://doi.org/10.3390/su16114433
14 R. Bastola, S. Shrestha, S. Mohanasundaram, and H. H. Loc: J. Water Clim. Change **15** (2024) 628. https://doi.org/10.2166/wcc.2023.521
15 B. Bidorn, S. Chanyotha, S. A. Kish, J. F. Donoghue, K. Bidorn, and R. Mama: Int. J. Sediment Res. (2015) 328.
16 H. D. Nguyen, C. P. Van, and A. D. Do: Earth Sci. Inf. **16** (2023) 1173. https://doi.org/10.1007/s12145-023-00954-4
17 H. Özdemir, M. Baduna Koçyiğit, and D. Akay: Stochastic Environ. Res. Risk Assess. **37** (2023) 4273. https://doi.org/10.1007/s00477-023-02507-z
18 M. S. Al-Sheriadeh and M. A. Daqdouq: Geomatics Nat. Hazards Risk **15** (2024) 2378991. https://doi.org/10.1080/19475705.2024.2378991
19 Y. Bhattarai, S. Duwal, S. Sharma, and R. Talchabhadel: Int. J. Digital Earth **17** (2024) 2313857. https://doi.org/10.1080/17538947.2024.2313857
20 S. Mangkhaseum, Y. Bhattarai, S. Duwal, and A. Hanazawa: Geomatics Nat. Hazards Risk **15** (2024) 2357650. https://doi.org/10.1080/19475705.2024.2357650

21 M. H. Hasan, A. Ahmed, K. M. Nafee, and M. A. Hossen: Ocean Coastal Manage. **236** (2023) 106503. https://doi.org/10.1016/j.ocecoaman.2023.106503

22 N. T. T. Linh, M. Pandey, S. Janizadeh, G. S. Bhunia, A. Norouzi, S. Ali, Q. B. Pham, D. T. Anh, and K. Ahmadi: Adv. Space Res. **69** (2022) 3301. https://doi.org/10.1016/j.asr.2022.02.027

23 M. U. Mia, T. N. Chowdhury, R. Chakrabortty, S. C. Pal, M. K. Al-Sadoon, R. Costache, and A. R. M. T. Islam: Land **12** (2023) 810. https://doi.org/10.3390/land12040810

24 R. Costache, T. T. Tin, A. Arabameri, A. Crăciun, I. Costache, A. R. M. T. Islam, M. Sahana, and B. T. Pham: Geocarto Int. **37** (2022) 13812. https://doi.org/10.1080/10106049.2022.2082558

25 Y. Li and H. Hong: J. Environ. Manage. **325** (2023) 116450. https://doi.org/10.1016/j.jenvman.2022.116450

About the Authors

Gen Long received his B.S. degree in vehicle engineering from Kunming University of Science and Technology, China, in 2012, and M.S. degree in disaster management from Naresuan University, Thailand, in 2022. He is currently a Ph.D. candidate in civil engineering at Naresuan University. His research interests are focused on disaster risk assessment optimization using machine learning techniques. (genl65@nu.ac.th)

Sarintip Tantanee received her B.Eng. degree in civil engineering from Chiang Mai University, Thailand. She then obtained her M.Eng. and Ph.D. degrees in water resources engineering from Kasetsart University, Thailand. From 2005 to 2009, she worked at the Electricity Generating Authority of Thailand (EGAT). She currently serves as the President of Naresuan University. Her research interests include water resources management, hydrology, and flood risk management. (sarintipt@nu.ac.th)

Korakod Nusit received his B.S. degree in civil engineering from Thammasat University, Thailand, in 2002, and his M.S. degree in engineering and applied geology from the Asian Institute of Technology, Thailand, in 2004. He later obtained his M.Eng. degree in geotechnical engineering from the National University of Singapore, Singapore, in 2011, and his Ph.D. in civil engineering from Curtin University, Australia, in 2017. He currently serves as the Associate Dean for Administration and Head of the Civil Engineering Department at Naresuan University. His research interests include numerical analysis in geotechnical engineering, transportation geotechnics, geological hazards, road materials, and road pavement design. (korakodn@nu.ac.th)

Pitikhate Sooraksa is a professor at the School of Engineering, King Mongkut's Institute of Technology Ladkrabang, Thailand. He received his B.Ed. (Hons) and M.Sc. degrees in physics from Srinakharinwirot University, Thailand, his M.S. degree from George Washington University, USA, in 1992, and his Ph.D. degree from the University of Houston, USA, in 1996, both in electrical engineering. His research interests include cyber-physical applications and rapid prototypes in robotics and AI. (pitikhate.so@kmitl.ac.th)